Optical Properties of Thermochromic Granular Films

Jørgen Vågan
Supervisor: Ingve Simonsen

August 10, 2015

Abstract

Abstract.. abstract.

1 Introduction

Today, in the light of global warming, the importance of reducing the amount released greenhouse gases into the atmosphere is more crucial now than ever. But because the use of fossil fuel is so well implemented in our society and constitute such an important energy source it is difficult to find replacements. However, through identifying inefficient systems that constitute the worst energy consumers and making use of technologies to increase their efficieny, a significant amount of the energy related carbon dioxide emissions may be reduced.

A relatively large portion of the energy consumption worldwide is in fact due to the building sector. Today the energy consumption of buildings in developed contries constitute about 30-40% of their total energy usage. In humid regions, this increases to roughly 30% to 50% [3, 4, 5]. In 2010, 41% of the primary energy of the U.S. (being the second largest energy consumer globally), accounting for 7% of the global energy use, were consumed by the building sector. This resulted in approximately 40% of the total energy-related carbon dioxide emmision in the US. For comparison, the building sector in China accounted for 18% of the CO2 emmision of the country, whereas worldwide the building energy consumption is the cause of 8% of the total carbon dioxide emmision. [2, 6]. Because this in total makes such a significant impact worldwide, it should motivate measures to be taken to reduce the building energy consumption, in order to reduce the related CO_2 emmisions. In addition to lowering the energy consumption, it would also lower the energy related costs related to the use of electricity. So reducing the overall building energy usage would have both economical and environmental benefits.

When considering the energy consumption of buildings, devices which stand for heating, ventilation and airconditioning (HVAC), which help to maintain a comfortable indoor climate, are actually accounting for much of the overall energy usage. HVAC devices are used to compensate for heat loss through the building's envelope (walls, roof, windows or any element separating the indoor from the outdoor) or excessive heating due to the thermal radiation from the sun. Together with lighting, HVAC were responsible for about 60% of the total building energy consumption in 2010 **(???in the U.S. or in general???)**. [2]. The approaches to increase the energy efficiency of buildings can be divided into two categories: active strategies, including improving HVAC systems and lighting of the building; and passive strategies, like improving the thermal properties of the building envelope. The latter includes measures like thermal insulation to walls, cool coatings on the roof tops or using windows with special coatings, altering the optical properties of the window [10, 11, 12, 13]. With the window actually being the most energy inefficient component of the building [6] **<- burde sjekkes, men har ikke tilgang (har ikke prøvd VPN**

enda , the measures focusing on improving the thermal properties of the window seems most reasonable, as they try to solve the seemingly worst issue regarding the energy efficiency of the building envelope. [1].

The thermal properties of the window depend mainly on the outdoor conditions, like shading, building orientation and type, in addition to the area of the window, its glass properties and glazing characteristics [8]. In window standards, the latter is the most important, because the glazing characteristics includes thermal transmittance coefficient [9]. ([1], s.354 avsnitt 2)
One way of improving the thermal efficieny of the window is to add some additional mechanism, allowing the window to change its properties to the environment. An example of such improved windows are called "smart-" or "intelligent windows" and will be discussed in the next section.

(The information for this section was gathered by [1]) **FJERN DETTE eller INKLUDER DETTE PÅ EN BEDRE MÅTE (om det er verdt å nevne)**
[2]

REFERENCES

[1] Kamalisarvestani M, Saidur R, Mekhilef S, Javadi FS. *Performance, materials and coathing technologies of thermochromic thin films on smart windows*, PressOrSomething?, Renewable and Sustainable Energy Reviews ?? 2013; 26:353-364 ?? **ER DETTE RIGKTIG?**

[2] *DoE U. Buildings energy databook* Energy Effucuebct & Renewable Energy Department 2011. **MÅ SJEKKES!**

[3] Al-Rabghi OM, Hittle DC. *Energy simulation in buildings: overview and BLAST example*. Energy Conversion and Management 2001;42(13):1623-35 **MÅ SJEKKES!**

[4] Wilde PD, Voorden MVD.C. *Providing computational support for the selection of energy saving building components*. Energy and Buildings 2004;36(8):749-58

[5] Kwak SY, Yoo SH, Kwak SJ. *Valuing energy-saving measures in residential buildings: a choice experiment study.* Energy Policy 2010; 38(1):673-7

[6] Hong T. *A close look at the China design standard for energy efficiency of public buildings*. Energy and Buildings 2009;41(4):426-35

[7] Baetens R, Jelle BP, Gustavsen A. *Properties, requirements and possibilities of smart windows for dynamic daylight and solar energy control in buldings: a state-of-the-art review*. Solar energy Materials and Solar Cells 2010;94(2):87-105

[8] Hassouneh K, Alshboul A, Al-Salaymeh A. Influence of windows on the energy balance of apartment buildings in Amman. Energy Conversion and Management 2010;51(8):1583-91.

[9] . Tarantini M, Loprieno AD, Porta PL. A life cycle approach to Green Public Procurement of building materials and elements: a case study on windows. Energy 2011;36(5):2473-82.

[10] Bojic M, Yik F, Sat P. Influence of thermal insulation position in building envelope on the space cooling of high-rise residential buildings in Hong Kong. Energy and Buildings 2001;33(6):569-81

[11] Cheung CK, Fuller R, Luther M. Energy-efficient envelope design for high rise apartments. Energy and Buildings 2005;37(1):37-48

[12] Synnefa A, Santamouris M, Akbari H. Estimating the effect of using cool coating on energy loads and thermal comfort in residential buildings in various climatic conditions. Energy and Buildings 2007;39(11):1167-74

[13] Sadineni SB, Madela S, Boehm RF. Passive building energy savings: a review of building envelope components. Renewable and Sustainable Energy Reviews 2011;15(8):3617-31

2 SMART/INTELLIGENT WINDOWS

Smart windows (or intelligent windows) is a type of windows that manages to regulate the transmitted solar radiation by changing its optical properties. The change in its optical properties can be obtained by adding a controllable absorbing layer on the surface of the glass. The ability of the smart window to optimize solar flux and daylight may help to reduce the electricity loads regarding heating, cooling and lighting. They should optimally also be able to adapt to the difference created by the seasons. E.g. summertimes have a different demand than wintertimes with respect to the thermal properties of the window. [4, 5, 8] Windows with such a switchable layer can be categorized into two systems: active and passive. The active switchable glazing systems require an external triggering mechanism and offers supplementary options compared to passive systems. An example of this is the electrochromic window. However, their dependency on a power supply and additional electronical curcuits makes them not as attractive as their passive counterparts. The passive devices do not require an external energy source, but switches automatically subject to environmental change. Examples of such devices are: photochromic windows reacting to light and thermochromic windows, which change in accordance to the temperature ([1]:[6]). As shown in Figure 2.1 the resulting energy load varies for the different window and glazing technologies. It also

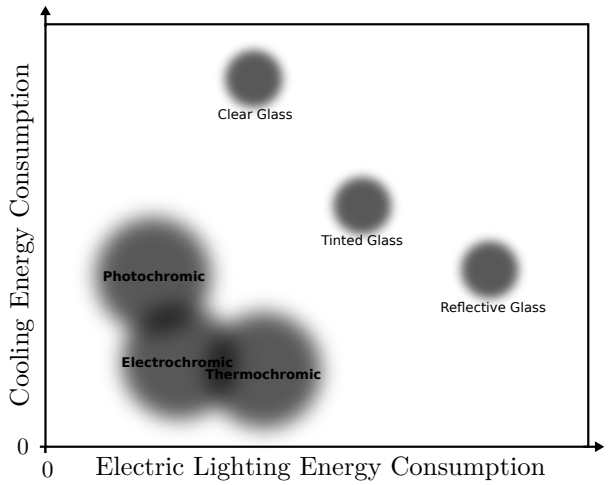

Figure 2.1: Comparison of the electric lighting energy and cooling energy consumption between different glazing types. Adapted from ([3],p.20).

demonstrates an important fact: even though using reflective glass would reduce cooling loads, a window should also be able to let visible light through! If the transmission of the visible spectrum is to low, it could cause the need for additional lighting, which again would increase the overall energy load ([1],12). Electrochromic and thermochromic windows usually result in lower cooling loads. In addition the electrochromic technology requires less energy for lighting. However, as argued in the review of Kamalisarvestani et al. [1], the necessity of wiring for electrochromic windows and the fact that the drawback regarding visible transmission in thermochromic windows can be solved by appropriate doping [13, p. 39](70), ensures the position of thermochromic windows as a good and actual low-priced alternative [14] **<-fikk ikke tilgang,prøv VPN**.

3 THERMOCHROMIC MATERIALS

The technology behind intelligent windows and its diversity, is based on materials that change their optical properties when subject to some external physical process. These materials are called chromic materials. The word chromic originates from the greek word "Chroma", which means color. If the induced change of optical properties results in changing the spectral reflectance in the visible spectrum, the material will change its color. *?CAN I SAY THIS WITHOUT A REFERENCE? ISN*T IT PRETTY OBVIOUS FROM ALL THE OTHER INFORMATION/ TAKEN FOR GRANTED? IT IS CORRECT RIGHT??* Chromic materials are again subdivided into categories dependent on what triggers their optical change, many of which have already been mentioned. For example, photochromic

and eletrochromic materials are two categories of chromic materials that changes their optical properties when subject to irradiation by light (photons) or an applied electric field, respectively. However, another subcategory is thermochromic materials and will be the category of interest in this assignment. ([2],1) The word thermochromic, compared to the "parent" material class, includes the extra word "Thermos", which is the greek word for warm or hot. As the name suggests, thermochromic materials change their optical properties (like color) in response to heat or, in other words, the change in temperature. ([1]:(74)<-ikke tilgang(prøv VPN),[7]). [8]

Typically, this change in color happens gradually over a range of temperatures. In this case it is called continuous thermochromism. Discontinuous thermochromism also occurs and involves a structural phase change at a certain characteristic "transition temperature" T_t. This phase change can be of first or second-order in nature, and may be reversible or irreversible ([2]:(1)).
Compounds like inorganic oxides, liquid cryctals ([2]:(2)), conjugated oligomers ([2]:(3)), leuco dyes ([2]:(4)) can exhibit thermochromic color changes reversibly. Thermochromic dyes however are usually based on organic compounds and show color changes on heating which are not reversible.

To explain the process behind the chromic behaviour, assume that the thermochromic material is initially in its cold state called the monoclinic state . Here it behaves as a semiconductor, being less reflective especially in the near-infrared(IR) region. Heating the material to a certain temperature, known as the transition temperature (as mentioned earlier), will make it change from the monoclinic state to a rutile state. In the rutile state (hot state) the material acts like a semi-metal, reflecting a wide range of solar radiation. This change of state is called metal-to-semiconductor transition (MST) [10, p. 4565] and is fully reversible, co-occured with large variations in both electrical and optical properties in the near-IR range [11]. **??? -> check if understood and correctly written. E.g. what is co-occured?**

Because of these interesting properties, thermochromic materials have become increasingly important, espacially through the use as "smart coatings" (for e.g. windows) as mentioned earlier. Some potential thin film candidates or smart windows include substances such as Fe_3O_4, $FeSi_4$, NbO_2, NiS, TiO_2 and VO_2. [8].

4 Thermochromic Windows

A thermochromic window, which has been meantioned serveral times earlier, is a window with a thermochromic glazing, allowing the window as a whole to adopt the optical properties of the thermochromic material. Figure 4.1 is a pictorial representation of the influence of the thermochromic coating on the window. Below the transi-

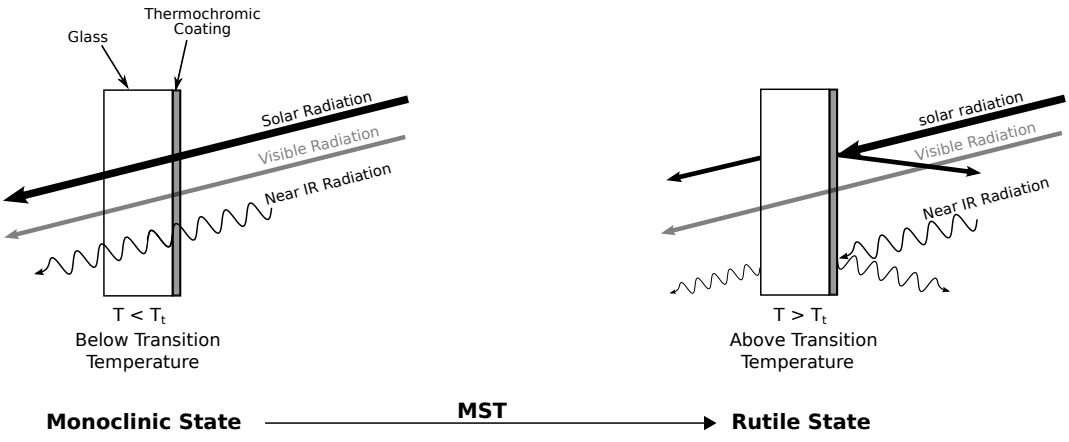

*Figure 4.1: Schematic representation of thermochromic materials applied as an intelligent window coating [**?**].*

tion temperature $T < T_t$, the window should transmit the solar thermal radiation, heating up the interior of the

building. If the temperature increases above the transition temperature T_t, the transmission of the thermal radiation should decrease significantly, lowering or removing the necessity of using cooling devices. For this to work, the transition temperature, which is usually much higher than room temperature, needs to be reduced down to a thermally comfortable level. This can be done by adding small quantities of a foreign material into the thermochromic material, a process called doping.

The ideal spectral modulation of the thermochromic coating is given in Figure 4.2 and shows how the cold state

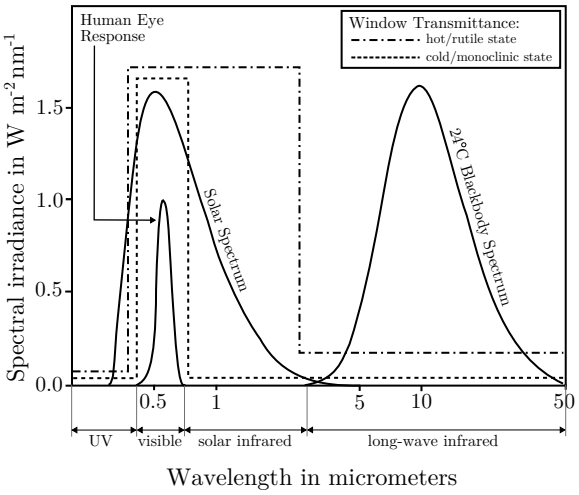

Figure 4.2: The spectral transmittance of a perfect thermochromic window, shown for both cold and hot environments (the monoclinic and rutile state, repsectively). Adopted from [1, p. 15]

should transmitt the majority of the solar radiation, here modeled as a black body spectrum. In addition it shows how the hot state should reflect as much of the infrared and solar radiation as possible without compromising the transmission of the visible spectrum. As mentioned earlier, if the transmission of daylight is poor, it would lead to an increase of the electrical load due to the accompanying additional lighting. [1] As discussed by Blackman [10], the optical transmission of the film is depending on the thickness of the film. Control of the film thickness is crucial. Excessive coating thicknesses may lead to too much blocking of the visual light, leaving the coating unsuitable for architectural application. In fact, for the transmission of visible light to be acceptable it should

Table 4.1: The ideal optical performance of thermochromic windows (taken from [1]) which adapted it from [12]

State	**Monoclinic/cold** ($T < T_t$)		**Rutile/hot** ($T > T_t$)	
Wavelength	Visible(%)	NIR (%)	Visible(%)	NIR (%)
Transmittance(T)	60-65	80	60-65	15
Reflectance(R)	17	12	17	77

be higher than 60%. The ideal performance of a thermochromic window is shown in Table **??**, showing that the modulation of visible should be the same for the monoclinic and rutile state and letting in more than 60% of the visible light.

5 VANADIUM DIOXIDE

5.1 DOPING OF VANADIUM DIOXIDE USING TUNGSTEN

(The switchable reflective device (or dynamic tintable window))

REFERENCES

[1] McCluney R, Center FSE. Fenestration solar gain analysis. Citeseer 1996.

[2] Kiri P, Hyett G, Binions R. Solid state thermochromic materials. Advances Material Letters 2010;1(2):20.

[3] Huovila P, Ala-Juusela M, Melchert L, Pouffary S. Buildings and climate change: status, challanges and opportunities. United Nations Environment Programme 2007.

[4] Dussault J-M, Gosselin L, Galstian T. Integration of smart windows into building design for reduction of yearly overall energy consumption and peak loads. Solar energy 2012;86(11):3405-16

[5] Jelle BP, Gustavsen A. Dynamic solar radiation control in buildings by applying electrochromic materials. Renewable Energy Conferance/Advanced materials technologies 2010; :133**er dette riktig?**

[6] Baetens R, Jelle BP, Gustavsen A. Properties, requirements and possibilities of smart windows for dynamic daylight and solar energy control in buildings: a state-of-the-art review. Solar energy materialsand solar cells 2010;94(2):87-105.

[7] Parkin IP, Manning TD. Intelligent thermochromic windows. Journal of Chemical Education 2006;83(3):393.

[8] White MA, LeBlanc M. Thermochromism in commercial products. Journal of Chemical Education 1999;76(9):1201,1204

[9] Lampert CM. Smart windows switch on the light. IEEE Circuits Devices Mag. 1992; 8(2):19

[10] Blackman CS, et al. Atmospheric pressure chemical vapour deposition of thermochromic tungsten doped vanadium dioxide thin films for use in architectural glazing. Thin Solid Films 2009;517(16):4565-70.

[11] Morin F. Oxides which show a metal-to-insulator transition at the Neel temperature. Physical Review Letters 1959;3(1):34-6

[12] Saeli M, et al. Energy modelling studies of thermochromic glazing. Energy and buildings 2010;42(10):1666-73.

[13] Kanu SS, Binions R. Thin films for solar control applications. Proceedings of the Royal Society of London series A 2010;466(2113):19-44

[14] Mlyuka N, Niklasson G, Granqvist CG. Thermochromic multilayer films of VO_2 and TiO_2 with enhanced transmittance. Solar Energy Materials and Solar Cells 2009;93(9):1658-7

6 THEORY BEHIND THE GRANFILM SOFTWARE

This section recapitulate the theoretical background behind GranFilm, a software used to calculate the optical properties of granular thin films.

6.1 THEORETICAL INTRODUCTION; FLAT SURFACE SCATTERING

Starting from basic electromagnetic theory, the simplest case of electromagnetic scattering is the transmission and reflection of light, hitting a flat, smooth interface between two different half-infinite media. The electric permittivity ε and magnetic permeability μ of the media are given with subscript + for the upper media, and − for the lower media, see Figure 6.1. Assuming that the incoming electromagnetic wave is a plane wave, the reflection

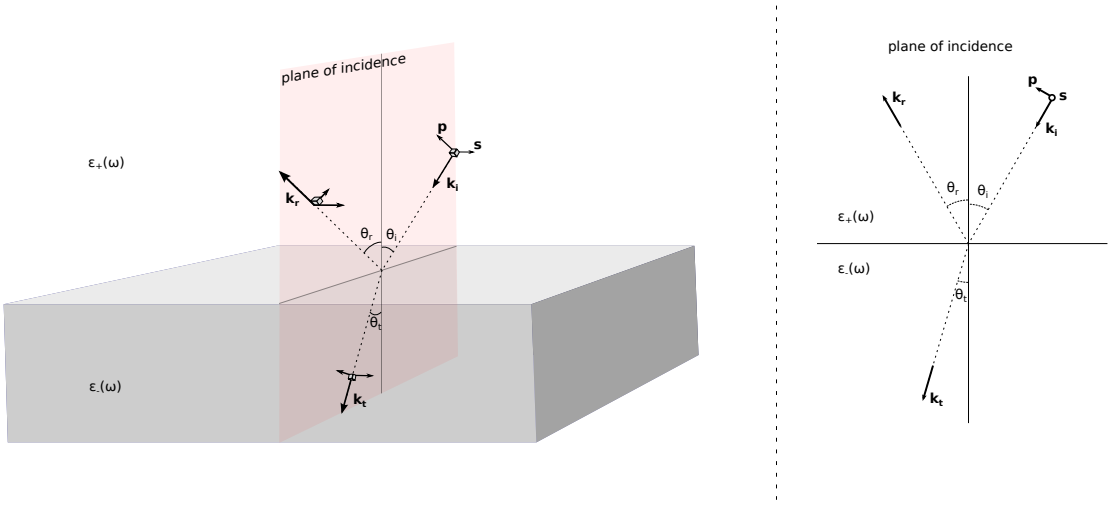

Figure 6.1: The reflection and transmission of an incident electromagnetic plane wave on a flat interface between two media. The dielectric functions for the upper and lower media are $\varepsilon_+(\omega)$ and $\varepsilon_-(\omega)$, respectively. The polarization direction $\boldsymbol{p}$ is the polarization parallel to or inside the place of incidence, while $\boldsymbol{s}$, which comes from the german word senkrecht meaning perpendicular, is the perpendicular polarization. The figure is adopted from ([1], p.125).

and transmission of the wave can be calculated from Maxwell's equations,

$$\nabla \cdot \boldsymbol{D} = \rho_f \qquad \nabla \times \boldsymbol{E} = -\frac{\partial \boldsymbol{B}}{\partial t} \tag{6.1a}$$

$$\nabla \cdot \boldsymbol{B} = 0 \qquad \nabla \times \boldsymbol{H} = \boldsymbol{J}_f + \frac{\partial \boldsymbol{D}}{\partial t}, \tag{6.1b}$$

which describe the general behavior of electromagnetic waves. Here the electric field $\boldsymbol{E}$, the electric displacement $\boldsymbol{D}$, the magnetic field $\boldsymbol{H}$ and the magnetic induction $\boldsymbol{B}$ are pairwise related through

$$\boldsymbol{D} = \varepsilon \boldsymbol{E}, \qquad \boldsymbol{H} = \frac{1}{\mu}\boldsymbol{B} \tag{6.2}$$

(assuming linear media) ([2], p.330). Further assuming that there is no free charge or free current at the interface, Maxwell's equation provide the boundary conditions ([2], p.333)

$$D_\perp^+ = D_\perp^- \qquad \boldsymbol{E}_\parallel^+ = \boldsymbol{E}_\parallel^- \tag{6.3a}$$

$$B_\perp^+ = B_\perp^- \qquad \boldsymbol{H}_\parallel^+ = \boldsymbol{H}_\parallel^-. \tag{6.3b}$$

($\perp$ and $\parallel$ denotes the perpendicular and parallel komponent with respect to the surface boundary. By enforcing these boundary conditions on the incident, reflected and transmitted waves, on the entire boundary, the reflection and transmission coefficients may be calculated. The coefficients are given by

$$R \equiv \frac{I_r}{I_i} \qquad T \equiv \frac{I_t}{I_i}, \tag{6.4}$$

$$\tag{6.5}$$

where $I_x, x \in [i,r,t]$ is the intensity or power per unit area stricking/leaving the interface for the incident, reflected and transmitted light, respectively ([2],p.386-391). The calculation can be found in any standard optics textbook *NEED OPTICS BOOK REFERENCE* and gives

$$R = r^2 \qquad T = \frac{n_- \cos\theta_t}{n_+ \cos\theta_i}. \tag{6.6}$$

$$\tag{6.7}$$

n_+ and n_- are the indices of refraction for the media above (+) and belov (-) the interface, while θ_i and θ_t gives the incident and transmitted lights direction with respect to the surface normal. The coefficients r and t are called the Frensel coefficients and their values depend on the polarization of the incident light. For the flat interface the coefficients take the form *NEED ANOTHER OPTICS BOOK REFERENCE*

$$r_s = \frac{n_+ \cos\theta_i - n_- \cos\theta_t}{n_+ \cos\theta_i + n_- \cos\theta_t} \qquad t_s = \frac{2n_+ \cos\theta_i}{n_+ \cos\theta_i + n_- \cos\theta_t}, \tag{6.8a}$$

$$r_p = \frac{n_- \cos\theta_i - n_+ \cos\theta_t}{n_+ \cos\theta_t + n_- \cos\theta_i} \qquad t_p = \frac{2n_+ \cos\theta_i}{n_+ \cos\theta_t + n_- \cos\theta_i} \tag{6.8b}$$

so the reflection and transmission are different for the two polarization directions, which can be seen in Figure 6.1.

6.2 Scattering On Rough Surfaces: Excess Fields And Surface Susceptibilities

When moving away from a flat surface, looking at a more complicated geometry of the boundary between the two media, the behavior of the dielectric function gets correspondingly diffucult. Situations like these might be encountered for rough surfaces or granular thin films, where the latter means that a foreign material is distributed as small island on top of a substrate. In these situations the calculation of the Fresnel coefficients turns increasingly complex ([1],p.125).

However, in order to calculate such complicated surfaces, Bedeaux and Vlieger ([1], (7-12)) developed an approach in which the exact knowledge of the electromagnetic fields close to the surface is not required. Their formalism is based on the notion of excess quantities. The excess fields are defined as the differene between the real fields and the bulk fields extrapolated to the surface, where the bulk field simply means the field given sufficiently far away from the scattering surface. E.g. for the electric field $E(r)$ the excess quantity is defined as

$$\boldsymbol{E}_{ex}(\boldsymbol{r}) = \boldsymbol{E}(\boldsymbol{r}) - \boldsymbol{E}^-(\boldsymbol{r})\theta(-z) - \boldsymbol{E}^+(\boldsymbol{r})\theta(z), \tag{6.9}$$

where $\theta(z)$ is the Heaviside function and the superscript $\pm$ are used to indicate the region above (+) and below (-) the dividing interface at $z = 0$. In addition, the optical frequency ω is implicitly included in the notation. Furthermore, the excess field is only significant close to the surface, since $\boldsymbol{E}(\boldsymbol{r},\omega) \to \boldsymbol{E}^{\pm}(\boldsymbol{r},\omega)$ when $z \to \pm\infty$. *???is this correct???* By integrating these excess fields along the z-axis, which is set normal to the surface,

$$\boldsymbol{D}^s_{\parallel}(\boldsymbol{r}) = \int_{-\infty}^{+\infty} dz\, \boldsymbol{D}_{ex,\parallel}(\boldsymbol{r}), \qquad E^s_z(\boldsymbol{r}) = \int_{-\infty}^{+\infty} dz\, E_{ex,z}(\boldsymbol{r}) \tag{6.10a}$$

$$\boldsymbol{B}^s_{\parallel}(\boldsymbol{r}) = \int_{-\infty}^{+\infty} dz\, \boldsymbol{B}_{ex,\parallel}(\boldsymbol{r}), \qquad H^s_z(\boldsymbol{r}) = \int_{-\infty}^{+\infty} dz\, H_{ex,z}(\boldsymbol{r}), \tag{6.10b}$$

and gathering them in a singular Dircac term, $\delta(z)$, located at the surface (z=0) (see Figure 6.2, the fields may be

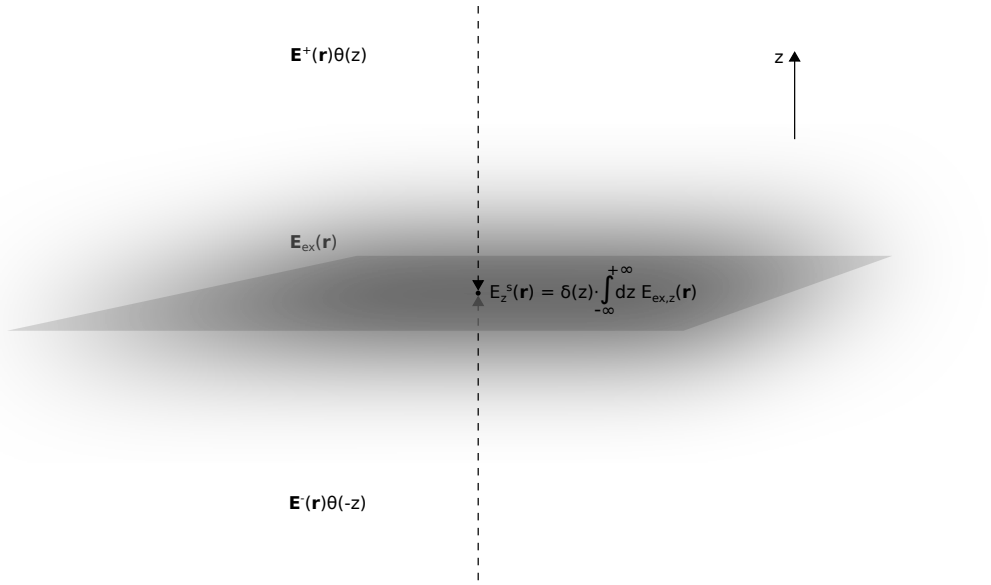

Figure 6.2: The excess fields are integrated over all values of z over the entire surface. Here this is vizualized for the eletric excess field, vizualized by the fog surrounding the surface, as the excess field, is only significant close to the surface. Note however that the excess field is complicated and not correctly represented by the fog. ([1], p.126).

rewritten on the form (here shown for just the electric field)

$$\boldsymbol{E}(\boldsymbol{r}) = \boldsymbol{E}^{-}(\boldsymbol{r})\theta(-z) + \boldsymbol{E}^{s}(\boldsymbol{r})\delta(z) + \boldsymbol{E}^{+}(\boldsymbol{r})\theta(z). \tag{6.11}$$

Demanding that the fields given by Eq. (6.11) fulfill the Maxwell equations ([1], (7-9)) one ends up with the following boundary conditions

$$\left[\boldsymbol{E}_{\parallel}^{+}(\boldsymbol{r}) - \boldsymbol{E}_{\parallel}^{-}(\boldsymbol{r})\right]\Big|_{z=0} = i\omega\hat{z}\times\boldsymbol{M}_{\parallel}^{s}(\boldsymbol{r}_{\parallel}) - \nabla_{\parallel}P_{z}^{s}(\boldsymbol{r}_{\parallel}) \tag{6.12a}$$

$$\left[D_{z}^{+}(\boldsymbol{r}) - D_{z}^{-}(\boldsymbol{r})\right]\Big|_{z=0} = -\nabla_{\parallel}\boldsymbol{P}_{\parallel}^{s}(\boldsymbol{r}_{\parallel}) \tag{6.12b}$$

$$\left[\boldsymbol{H}_{\parallel}^{+}(\boldsymbol{r}) - \boldsymbol{H}_{\parallel}^{-}(\boldsymbol{r})\right]\Big|_{z=0} = i\omega\hat{z}\times\boldsymbol{P}_{\parallel}^{s}(\boldsymbol{r}_{\parallel}) - \nabla_{\parallel}M_{z}^{s}(\boldsymbol{r}_{\parallel}) \tag{6.12c}$$

$$\left[B_{z}^{+}(\boldsymbol{r}) - B_{z}^{-}(\boldsymbol{r})\right]\Big|_{z=0} = -\nabla_{\parallel}\boldsymbol{M}_{\parallel}^{s}(\boldsymbol{r}_{\parallel}), \tag{6.12d}$$

which is derived in Vlieger and Bedaux's *Optical Properties of Surfaces* (p.21). Here $\nabla_{\parallel}$ is the nabla operator parallel to the surface, while z denotes the vector component in the direction normal to the surface at $z = 0$. In addition, the quantities with superscript s are the so-called excess polarization and magnetization densities

$$\boldsymbol{P}^{s}(\boldsymbol{r}_{\parallel}) = \left(\boldsymbol{D}_{\parallel}^{s}(\boldsymbol{r}_{\parallel}),\ -\varepsilon_{0}E_{z}^{s}(\boldsymbol{r}_{\parallel})\right) \tag{6.13a}$$

$$\boldsymbol{M}^{s}(\boldsymbol{r}_{\parallel}) = \left(\boldsymbol{B}_{\parallel}^{s}(\boldsymbol{r}_{\parallel}),\ -\mu_{0}H_{z}^{s}(\boldsymbol{r}_{\parallel})\right), \tag{6.13b}$$

Here, in Eq.(6.13), the quantities on the right hand side are the integrated excess fields. Even though Maxwell's equations have been included, demanding that the fields follow the boundary conditions of (6.12), they do not uniquely determine the physical situation. Maxwell's equations in matter (6.1), given in Section 6.1, includes $\boldsymbol{E}$ and $\boldsymbol{D}$, together with $\boldsymbol{B}$ and $\boldsymbol{H}$, , but does not state how they depend on eachother. In other words, Eq. (6.1) does not contain more information than Maxwell's equations given in free space. So, to fully explain how the fields interact with material and the interface, constitutive relations characteristic to the surface must be given

(like the relations in Eq.(6.2) given for the flat interface example) ([2], p. 330). The constitutive relations link the interfacial polarisation and magnetization density $\left(\boldsymbol{P}^s(\boldsymbol{r}_\parallel)\right.$ and $\left.\boldsymbol{M}^s(\boldsymbol{r}_\parallel)\right)$ and the bulk fields extrapolated to the surface. If the pertubed surface layer thickness d is negligible compared to the optical wavelength λ, the excess fields are only significant or non-negligible close to the surface, which followed from the notation for the excess fields assumed earlier in Eq. (6.9). Because of this, the constitutive relations are local and the extrapolated bulk fields may be written on the form $\boldsymbol{E}_{\parallel,\Sigma} = \left\{\boldsymbol{E}_\parallel^+(\boldsymbol{r}_\parallel) + \boldsymbol{E}_\parallel^-(\boldsymbol{r}_\parallel)\right\}/2$. For simplisity we restrict our discussion to non-magnetic materials, i.e. that $\boldsymbol{M}^s(\boldsymbol{r}_\parallel) = 0$. The simplest constitutive relation can be written on the form

$$\boldsymbol{P}^s(\boldsymbol{r}_\parallel) = \xi_e^s\left[\boldsymbol{E}_{\parallel,\Sigma}(\boldsymbol{r}_\parallel),\ -D_{z,\Sigma}(\boldsymbol{r}_\parallel)\right]. \tag{6.14}$$

By further assuming that the interface is homogeneous and isotropic, the interfacial tensor reduces to a diagonal matrix:

$$\xi_e^s = \begin{bmatrix} \gamma & 0 & 0 \\ 0 & \gamma & 0 \\ 0 & 0 & \beta \end{bmatrix}, \tag{6.15}$$

With the first order surface susceptibilities γ and β. The reason why they are called first order susceptibilities is because the discussion above limits the dependence between the integrated excess quantities and the extrapolated bulk fields to a local relation (second order would require a spatial relation). In fact, even though they are not included in this discussion, GranFilm also takes account for the non-local dependence, described by the constitutive coefficients of second order δ and τ ([1], (7,15)). These quantities are of the order d/λ smaller than the first order coefficients. Linear combinations of δ and τ together with the first order susceptibilities γ and β can construct invariants, which are independent of the choice of the separation surface. Furthermore, the Fresnel quantities, which all are measurable, are also independent of where we choose to put the surface in our coordinate system and can be uniquely expressed as a function of these constructed invariants. This discussion will continue to only consider the first order susceptibilities γ and β, which are the dominating factors when considering granular layers consisting of metallic islands.

6.3 The Fresnel coefficients

Using the same method as for the flat Fresnel surface, the Fresnel coefficients in terms of the surface susceptibilities can be derived. The derivation is tedious and will not be done here. It can however be found in Bedeaux and Vlieger's book ([3], p.45) ([6],p.10). In addition to the classical approach, the excess field boundary conditions (6.12), together with the constitutive relation between the interface and the extrapolated bulk fields (6.14). A property of this approach, is that the complicated surface, approximated by the pertubed layer, does not change the fact of *Snell's law*, which pops out of the boundary conditions when calculating the classical flat surface problem ((**??**), p388). In other words,

$$\theta_i = \theta_r \tag{6.16a}$$

$$n_+ \sin\theta_i = n_- \sin\theta_t. \tag{6.16b}$$

is still used to find the angle of incidence θ_i, reflection θ_r and transmission θ_t. They are, so to speak, unmodified by the pertubed layer. However, the Fresnel coefficients, which decide the reflection and transmission amplitudes, do depend on the pertubed layer through the surface susceptibilities. For s-polarization, the resulting Fresnel coefficients are given by

$$r_s(\omega) = \frac{n_-\cos\theta_i - n_+\cos\theta_t + i(\omega/c)\gamma}{n_-\cos\theta_i + n_+\cos\theta_t - i(\omega/c)\gamma} \tag{6.17a}$$

$$t_s(\omega) = \frac{2n_-\cos\theta_i}{n_-\cos\theta_i + n_+\cos\theta_t - i(\omega/c)\gamma}. \tag{6.17b}$$

For p-polarization the expressions are more complicated

$$r_p(\omega) = \frac{\kappa_-(\omega) - i(\omega/c)\gamma\cos\theta_i\cos\theta_t + i(\omega/c)n_-n_+\varepsilon_-\beta\sin^2\theta_i}{\kappa_+(\omega) - i(\omega/c)\gamma\cos\theta_i\cos\theta_t - i(\omega/c)n_-n_+\varepsilon_-\beta\sin^2\theta_i}, \tag{6.18a}$$

$$t_p(\omega) = \frac{2n_-\cos\theta_i\left[1 + (\omega/2c)^2\varepsilon_-\gamma\beta\sin^2\theta_i\right]}{\kappa_+(\omega) - i(\omega/c)\gamma\cos\theta_i\cos\theta_t - i(\omega/c)n_-n_+\varepsilon_-\beta\sin^2\theta_i}, \tag{6.18b}$$

where there has been introduced two quantites $\kappa_\pm$ defined as

$$\kappa_\pm = \left[n_+ \cos\theta_i \pm n_- \cos\theta_t\right]\left[1 - \frac{\omega^2}{4c^2}\varepsilon_- \gamma\beta \sin^2\theta_i\right]. \tag{6.18c}$$

The simplicity of the expressions for s-polarization (6.17) compared to p-polarization (6.18), is due to the fact that s-polarized light only manages to excite modes parallel to the surface. This is reflected in the equations by the fact that $r_s(\omega)$ and $t_s(\omega)$ only depend on the parallel surface susceptibility γ. P-polarized light on the other hand, can excite modes both parallel and perpendicular to the interface, and gives rise to the increased complexity of $r_p(\omega)$ and $t_p(\omega)$, with the dependency of both γ and β.
If the surface susceptibilities in the expressions above are set to zero ($\gamma = \beta = 0$), this means that the perturbation from the flat interface, caused by the granular layer, disappears and the Fresnel coefficients, (6.17) and (6.18), reduce to the flat Fresnel coefficients, (6.8a) and (6.8b), respectively.

In addition to the source frequency ω, the refractive indices $n_\pm$ and the incident angle θ_i are input parameters. The three latter provide, through Snell's law (6.16) as mentioned above, the calculation of the angle of transmittance θ_t. However, the surface susceptibilies γ and β are not known and, in order to calculate the Fresnel coefficients for the pertubed surface layer, these quantities must be found.

6.4 Surface susceptibilities of island layer

To this point, there has been no assumptions regarding the geometrical nature of the surface layer. The kind of layer to be considered is a discontinuous thin film of nm-sized island, constituting a granular layer. If the islands are much smaller than the optical wavelength, the scattering from the granular film will be negligible and the resulting angular distribution of light will be similar to that of a flat interface ([**?**].p.11, (2,p.99) **<- fjern Lie, sjekk og bruk kilde?**). In this case, the density of islands, or the number of island per unit surface area ρ, together with their ability to react to the applied field, , decide the surface polarization density $\boldsymbol{P}^s(\boldsymbol{r}_\parallel)$

$$\gamma = \rho\alpha_\parallel \qquad\qquad \beta = \rho\alpha_\perp \tag{6.19}$$

The surface's ability to react to the applied field is called the polarizability α of the surface, where $\alpha_\parallel$ is the polarizability parallel to the surface, while $\alpha_\perp$ is perpendicular to the surface. ([**?**], (7,11,12,24))

In other words, the optical properties in this situation is essentially driven by the polarizability of the island. The *GranFilm* software, supports the caulculation of both truncated spheres and truncated oblate or prolate spheroids. These two particle shapes can represent a great number of experimental situations, with the latter including shapes ranging from discs to needles. ([1], p.128)

To calculate the surface polarizabilities, the first step is to solve Laplace's equation for the electrostatic potential

$$\nabla^2\Psi(\boldsymbol{r}) = 0 \tag{6.20}$$

in the quasi-static limit. An easy way to understand the quasistatic limit of Maxwell's equations is, as stated in ([4],p.238), to let $c \to \infty$, which would neglect all effects due to time retardation. This means that any charge or current distribution at any instant in time, would decide the resulting fields at the same instant, in all of space. In other words: the effect of the sources will be instantaneous. The validity of the result depends on the distance to the source and how fast the fields are fluctuating, making the approximation valid if the distances are sufficiently short or if the fluctuations of the fields are sufficiently slow ([2], p.308-309). In the case of the granular film, the approximation is valid for sub-wavelength-sized island, in correspondence to the assumption of the layer thickness compared to the wavelength of the incident light.
Assuming spherical island geometry, the potential can be expanded in a multipolar basis of seperable solutions to (6.20)

$$\Psi(\boldsymbol{r}) = \sum_{lm} A_{lm} r^{-l-1} Y_l^m(\theta,\phi) + \sum_{lm} B_{lm} r^l Y_l^m(\theta,\phi) \tag{6.21}$$

Here (r, θ, ϕ) are the spherical coordinates centered at the expansion point, A_{lm} and B_{lm} are the multipole expansion coefficients and $Y_l^m(\theta,\phi)$ are the spherical harmonics. The coordinate system for the expansion is given in Figure 6.3, with μ denoting the center of expansion, which may be centered at the truncated sphere or

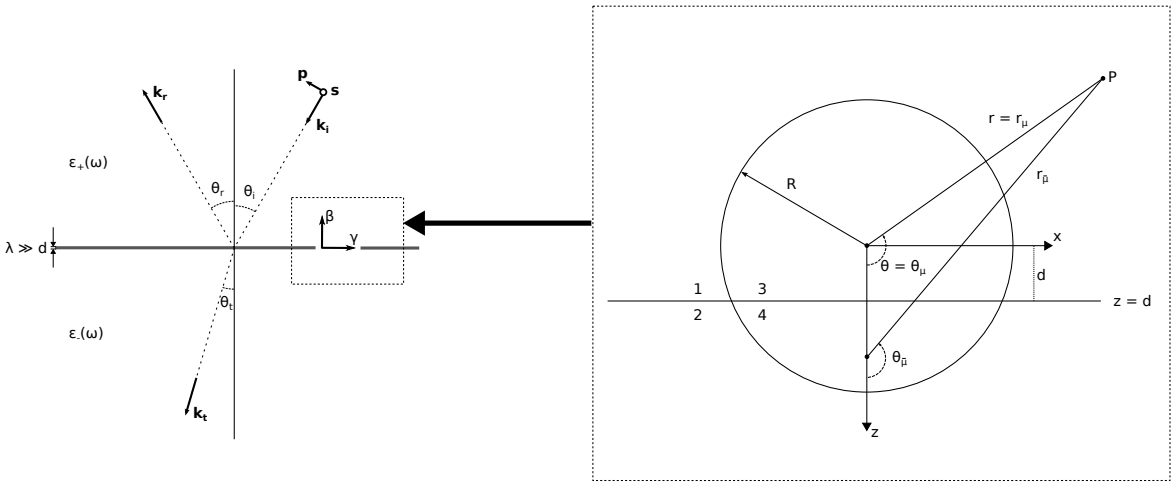

Figure 6.3: To the left: the transmission and reflection of a pertubed surface layer with thickness d, which is assumed to be much smaller than the optical wavelength λ of the incoming wave. The reflection and transmission amplitudes depend on the surface susceptibilities. The first order surface susceptibilities, γ and β, describe the ability of the surface to polarise in the parallel or perpendicular direction. These coefficients can be calculated from evaluating the geometry of the trunctated spheres (shown to the right), making up the granular thin film ([1], p.126). Adopted from ([1], p.125)

varied along the vertical symmetry axis. To deal with the boundary truncating the sphere, the classical image technique is used ([1],(13)). This is done by having a image expansion center located at the opposite side of the surface, compared to μ, inside the substrate. The image expansion point is denoted by $\bar\mu$. **Should I also mention t_r and the difference between $t_r > 0$ and $t_r < 0$?** As shown in Figure 6.3, mathematical approach assumes 4 different media, even though region 4 is part of the substrate. When specifying the material in the software region 2 and 4, which constitute the substrate, are usually set to be the same. Using Eq.(6.21) to expand the potential around the expansion center and the image, the potential in the different regions take the form:

$$\Psi_1(\boldsymbol{r}) = \Psi_i(\boldsymbol{r}) + \sum_{lm}^{l\neq 0} A_{lm} r_\mu^{-l-1} Y_l^m(\theta_\mu,\phi_\mu) + \sum_{lm}^{l\neq 0} A^r_{lm} r_{\bar\mu}^{-l-1} Y_l^m(\theta_{\bar\mu},\phi_{\bar\mu}) \tag{6.22a}$$

$$\Psi_2(\boldsymbol{r}) = \Psi_t(\boldsymbol{r}) + \sum_{lm}^{l\neq 0} A^t_{lm} r_\mu^{-l-1} Y_l^m(\theta_\mu,\phi_\mu) \tag{6.22b}$$

$$\Psi_3(\boldsymbol{r}) = \psi_0(\boldsymbol{r}) + \sum_{lm}^{l\neq 0} B_{lm} r_\mu^{l} Y_l^m(\theta_\mu,\phi_\mu) + \sum_{lm}^{l\neq 0} B^r_{lm} r_{\bar\mu}^{l} Y_l^m(\theta_{\bar\mu},\phi_{\bar\mu}) \tag{6.22c}$$

$$\Psi_4(\boldsymbol{r}) = \psi_0(\boldsymbol{r}) + \sum_{lm}^{l\neq 0} B^t_{lm} r_\mu^{l} Y_l^m(\theta_\mu,\phi_\mu) \tag{6.22d}$$

Here, the $r^l\big|_{l=0}$ terms of the expansion are constant and have been extracted, giving the value $\psi_0(\boldsymbol{r})$ inside the sphere (region 3 and 4, see Fig.6.3). The negative terms $r^{-1-l}\big|_{l=0} = r^{-1}$ represents free charge, wich has been assumed to be zero, and are removed. Outside the sphere (region 1 and 2) the potential is set to zero, simply because the potential reference point can be chosen freely. In addition to the $l = 0$-terms, the incident field gives rise to the potential $\Psi_i(\boldsymbol{r})$. Some of the incident light is transmitted directly into the substrate and the resulting scalar field is given by $\Psi_t(\boldsymbol{r})$. **Burde kanskje ta med at $\Psi_i(\boldsymbol{r})$, $\Psi_t(\boldsymbol{r}) \sim -\boldsymbol{r}\cdot\boldsymbol{E}_0$. Men forstår det ikke...(se evt. M.thesis Leif Amind Lie)** Comparing Eqs. (6.22) to Eq. (6.21), note that all the r^l-terms in region 1 and 2, r^{-l-1}-terms in region 3 and 4 are removed due to the divergence of the potential as $r \to \infty$ and $r \to 0$, respectively.

The boundary conditions for the electric potential is given by ([2], p.89-90)

$$\varepsilon_i(\omega)\,\partial_n\Psi_i(\boldsymbol{r}) = \varepsilon_j(\omega)\,\partial_n\Psi_j(\boldsymbol{r}) \qquad \Psi_i(\boldsymbol{r}) = \Psi_j(\boldsymbol{r}) \tag{6.23}$$

where $\partial_n = \hat{n}\cdot\nabla$ is the derivative with respect to the normal direction $\hat{n}$ to the boundary surface, and the indicies $i,j \in \{1,2,3,4\}$, $i \neq j$ denotes the different media included at the different boundaries. From the boundary conditions the relation between the multipole coefficients are found

$$A^r_{lm} = (-1)^{l+m}\frac{\varepsilon_1-\varepsilon_2}{\varepsilon_1+\varepsilon_2}A_{lm} \tag{6.24a}$$

$$A^t_{lm} = \frac{2\varepsilon_1}{\varepsilon_1+\varepsilon_2}A_{lm} \tag{6.24b}$$

$$B^r_{lm} = (-1)^{l+m}\frac{\varepsilon_3-\varepsilon_4}{\varepsilon_3+\varepsilon_4}B_{lm} \tag{6.24c}$$

$$B^t_{lm} = \frac{2\varepsilon_3}{\varepsilon_3+\varepsilon_4}B_{lm}. \tag{6.24d}$$

However, there are still 4 unknowns for each multipole order (every configuration of l and m). By using the orthogonality of the spherical harmonics $Y^m_l(\theta,\phi)$ to treat the boundary of the sphere, called the weak formulation of the boundary conditions, give two infinite linear systems for the multipolar coefficients A_{lm} and B_{lm} for $l = 1$, $m = 0,\pm1$. To solve this system in practive, some cut-off value $l = M$ for the expansion is set. Based on investigations by Simonsen and Lazzari [5] a truncation at $M = 16$ appeared to be sufficient in most cases. This result is based on post-checking the boundary condition for the potential and the normal displacement at the surface; and convergence tests of the first term of the multipolar expansion. Keep in mind, that for cases like spherical caps (truncated at the upper hemisphere) or entire spheres on top of a substrate the convergence could be slower, requiring a truncation $M > 16$. Finally, knowing the first multipolar coefficients the polarizability of the islands can be found

$$\alpha_\perp \simeq A_{10} \qquad \alpha_\parallel \simeq A_{11}. \tag{6.25}$$

The first $l = 0$ terms of region 1 A_{lm} are representing the dipole contribution, which dominates in the far-field limit ([**?**]: Bedeaux and Vlieger->(2), **Må sjekkes!**).

6.5 Inter-island coupling; collective contribution

So far, the discussion has only included the response of a single island and would perhaps give resonable result in the low coverage limit. However, this would lead to an increase in error for larger covarages and create the need for a correction due to the increasing island-island interaction ([**?**], p. 20). By assuming that the island are sufficiently close to one another such that their mutual separation is negligible compared to the optical wavelength, a correction to the low-coverage result can be obtained. In this limit, the islands would be excited by the same incident field and have similar responses to the field. Assuming a dipole response, the islands would be affected by the dipole fields excited in the neighboring particles. If the spheres are truncated by the substrate through their lower hemisphere, the modified polarizabilities compared to the isolated polarizatilities, $\alpha_\perp, \alpha_\parallel$, become

$$\alpha^{\text{mod}}_\perp = \frac{\alpha_\perp}{1-2\alpha_\perp I^{20}_\perp} \qquad \alpha^{\text{mod}}_\parallel = \frac{\alpha_\parallel}{1+2\alpha_\parallel I^{20}_\parallel}. \tag{6.26}$$

The defined functions in the correction are called the interaction functions

$$I^{20}_\perp = \frac{1}{\sqrt{20\pi}L^3\varepsilon_-}\left[S_{20} - \left(\frac{\varepsilon_- - \varepsilon_+}{\varepsilon_- + \varepsilon_+}\right)\tilde{S}^r_{20}\right] \tag{6.27a}$$

$$I^{20}_\parallel = \frac{1}{\sqrt{20\pi}L^3\varepsilon_-}\left[S_{20} + \left(\frac{\varepsilon_- - \varepsilon_+}{\varepsilon_- + \varepsilon_+}\right)\tilde{S}^r_{20}\right], \tag{6.27b}$$

where

$$S_{20} = \sum_{i\neq 0}\left(\frac{L}{r}\right)^3 Y^0_2(\theta,\phi)\Big|_{r=R_i} \tag{6.28a}$$

$$S^r_{20} = \sum_{i\neq 0}\left(\frac{L}{r}\right)^3 Y^0_2(\theta,\phi)\Big|_{r=R^r_i} \tag{6.28b}$$

are the direct and image lattice sums, describing the interaction with the other direct and image dipoles, respectively. L stands for the lattice constant. The $i = 0$ term in the summation gives the contribution from the interaction with the corresponding image of an island. This is taken into account when calculating the isolated response and is therefore not needed in Eq.(6.28). The validity of the dipolar approximation was tested by Lazzari and Simonsen for hemispherical silver islands layed out in a hexagonal pattern on a MgO substrate ([1], p.129-130). The polarizabilities were computed for $M = 16$ and showed that the relative error of the dipole approximation compared quadrupole approximation is $sim1\%$ up to 40% coverage, which is higher than the interesting limits encountered in experiments.

the fields above $\boldsymbol{E}^{+}(\boldsymbol{r})$ and below $\boldsymbol{E}^{-}(\boldsymbol{r})$ the interface can be calculated for a incident place wave (same goes for $\boldsymbol{B}$, $\boldsymbol{D}$ and $\boldsymbol{H}$). So far, the boundary between the two half-infinite media has been considered to be a sharp, flat discontinuity in $\varepsilon(z)$ and $\mu(z)$. As soon as the surface roughness, thickness and/or impurities are taken into acount, the complexity of the problem increases.

Føler jeg burde ha referance til masteroppgaven jeg har sett på også... er dette en grei ting å gjøre?

REFERENCES

[1] Lazzari R, Simonsen I. GranFilm: a software for calculating thin-layer dielectric properties and Fresnel coefficients. Thin Solid Films 2002;419:124-136 *ER DETTE RIKTIG?*

[2] Griffiths DJ. Introduction to electrodynamics, third edition. Pearson, international edition 2008.

[3] Bedeaux D, Vlieger J. Optical properties of surfaces. Imperial College Press, second edition 2004.

[4] Larsson J. Electromagnetics from a quasistatic perspective. American Association of Physics Teachers, 2007. **??Er denne riktig???**

[5] Simonsen I, Lazzari R. Jupille J, Roux S. Numerical modeling of the optical response of supported metallic particles. Physical Review B, 61(11):7722-7733, 2000.

[6] Lie LA, Simonsen I. Optical properties of a thin film of coated, truncated spheres. NTNU 2010. Imperial College Press, second edition 2004.

7 METHOD

8 RESULTS

9 DISCUSSION

10 CONCLUSION

11 INTRODUCTION TO GRANFILM

This section is included as a brief summary of the practical situations one encounter when using GranFilm. Even though the software provides the information required and would be self-explanatory for some, this would be for the less experienced reader to avoid any unecessary confusion.

11.1 SOFTWARE OVERVIEW

GRANFILM is a program written in FORTRAN 90 and serves as a tool for simulating and interpreting optical spectra from surfaces or thin films. The program takes in parameters specifying the incoming angle, polarization and energy range of the incoming plane wave, in addition to the radius and truncation ratio t_r of the sphere, the materials for region 1,2,3 and 4, the arrangement of the islands and finally the multipole order M.

To give the correct optical response of the specified materials, GRANFILM is connected to a dielectric database, containing data for metals, semiconductors and dielectrics. The datafiles for the different materials contain the real and complex index of refraction, n and k, respectively, with the first line of the file containing 4 values, which specifies

1. the unit, telling that it is a function of
   - `unit = 1`: energy in electron volts, or
   - `unit = 2`: wavelength in micrometers;
2. starting value `x1` of the domain (in units corresponding to the previous point);
3. end value of domain `x2`;
4. the number of datapoints `N`.

So ".nk-files" will be on the form: An example is "mgo.nk" in electron volts, a start value of 0.65eV, end value of 10eV and containing 400 data points:

- Source: giving the characteristics of the incident plane wave.
  - Theta0, Phi0: incident angles [°]
  - Polarization: 's' (senkrecht-polarized) / 'p' (parallel-polarized)
  - Energy_Range: the range of energies of the incident light. **Note: this range must be within the range of [x1,x2] for the input values for the refractive index, given in the '.nk' file!**
- Geometry:
  - Radius:
- Interaction:
  - coverage

12 Additional Theory

12.1 Complex permittivity and refractive index (From wikipedia) don't use, LACKING REFERENCES!

Complex electric permittivity:

$$\hat{\varepsilon}_r(\omega) = \frac{\hat{\varepsilon}(\omega)}{\varepsilon_0} \tag{12.1}$$

where

$$\hat{\varepsilon}_r(\omega) = \varepsilon_r(\omega) + i\tilde{\varepsilon}_r(\omega) \tag{12.2}$$

$$= \varepsilon_r(\omega) + i\frac{\sigma}{\omega\varepsilon_0} \tag{12.3}$$

The complex refractive index $\hat{n}$ is given by

$$\hat{n} = \sqrt{\hat{\varepsilon}_r}, \tag{12.4}$$

when the magnetic properties are neglected ($\mu_r = 1$). From this, an expression for the complex refractive index $\hat{n} = n - \boldsymbol{i}\kappa$ can be found:

$$\hat{\varepsilon}_r = \hat{n}^2 \tag{12.5}$$

$$\varepsilon_r + \boldsymbol{i}\tilde{\varepsilon}_r = (n + \boldsymbol{i}\kappa)^2 \tag{12.6}$$

$$\varepsilon_r + \boldsymbol{i}\tilde{\varepsilon}_r = n^2 - \kappa^2 + \boldsymbol{i}2n\kappa \tag{12.7}$$

giving

$$\varepsilon_r = n^2 - \kappa^2 \qquad\qquad \tilde{\varepsilon}_r = 2n\kappa. \tag{12.8}$$

Taking the absolute value or modulus of the relative permettivity

$$|\hat{\varepsilon}_r| = \sqrt{\varepsilon_r^2 + \tilde{\varepsilon}_r^2} \tag{12.9}$$

$$|\hat{\varepsilon}_r| = \sqrt{(n^2 - \kappa^2)^2 + (2n\kappa)^2} \tag{12.10}$$

$$|\hat{\varepsilon}_r|^2 = (n^4 - 2n^2\kappa^2 + \kappa^4) + 4n^2\kappa^2 \tag{12.11}$$

$$|\hat{\varepsilon}_r|^2 = n^4 + 2n^2\kappa^2 + \kappa^4 \tag{12.12}$$

$$|\hat{\varepsilon}_r|^2 = (n^2 + \kappa^2)^2 \tag{12.13}$$

$$|\hat{\varepsilon}_r| = n^2 + \kappa^2 \tag{12.14}$$

and adding or substracting the real part of the permittivity, gives

$$|\hat{\varepsilon}_r| + \varepsilon_r = (n^2 + \kappa^2) + (n^2 - \kappa^2) = 2n^2 \tag{12.15}$$

$$|\hat{\varepsilon}_r| - \varepsilon_r = (n^2 + \kappa^2) - (n^2 - \kappa^2) = 2\kappa^2. \tag{12.16}$$

Refomulating the expression gives the real and imaginary parts of $\hat{n}$

$$n = \sqrt{\frac{|\hat{\varepsilon}_r| + \varepsilon_r}{2}} = \sqrt{\frac{|\hat{\varepsilon}| + \varepsilon}{2\varepsilon_0}} \tag{12.17}$$

$$\kappa = \sqrt{\frac{|\hat{\varepsilon}_r| - \varepsilon_r}{2}} = \sqrt{\frac{|\hat{\varepsilon}| - \varepsilon}{2\varepsilon_0}} \tag{12.18}$$

12.2 Polarizability. Don't use, lacking references

When a neutral atom is placed in an electric field $\boldsymbol{E}$, the field tries to rip the atom apart by pushing the nucleus in the direction of the field and the electrons in the opposite direction. Because of the attraction between the positive and negative charge within the atom, an equilibrium displacement of the electrons compared to the nucleus is achieved, leaving the atom polarized and giving it a dipole moment. The dipole moment can be approximated by

$$\boldsymbol{p} = \alpha \boldsymbol{E}, \tag{12.19}$$

where α is the atomic polarizability and may depend on the detailed structure of the atom. For more complicated situations, like an asymmetrical molecule, the gained dipole moment of the molecule does not necessarily have to be in the same direction as the applied electric field. In such a case, the scalar polarizability in the expression above is replaced by a polarizability tensor

$$\boldsymbol{\alpha} = \begin{bmatrix} \alpha_{xx} & \alpha_{xy} & \alpha_{xz} \\ \alpha_{yx} & \alpha_{yy} & \alpha_{yz} \\ \alpha_{zx} & \alpha_{zy} & \alpha_{zz} \end{bmatrix}. \tag{12.20}$$

In this way, an applied eletric field induces many dipole moments in a material. In addition, any polar molecules will be subject to a torque, aligning it to the direction of the field. These two mechanisms leads to the polarization $\boldsymbol{P}$ of the material

$$\boldsymbol{P} = \text{dipole moment per unit volume} = \varepsilon_0 \chi_e \boldsymbol{E}. \tag{12.21}$$

In the above expression, there has been assumed a linear dielectric media, where χ_e is the electric susceptibility and depends on the microscopic structure of the material, in addition to the external temperature ([2],p.160-166, 179)

12.3 The electric potential, Laplace's equation and the Uniqueness Theorem

The usual task of electrostatics is to ompute the electric field $\boldsymbol{E}$ given a stationary charge distribution $\rho \boldsymbol{r}$

$$\boldsymbol{E}(\boldsymbol{r}) = \frac{1}{4\pi\varepsilon_0} \int \frac{\hat{\boldsymbol{d}}(\boldsymbol{r}')}{d(\boldsymbol{r}')^2} \rho(\boldsymbol{r}') d\boldsymbol{r}' \tag{12.22}$$

$$= \frac{1}{4\pi\varepsilon_0} \int \frac{\boldsymbol{r} - \boldsymbol{r}'}{\left|\boldsymbol{r} - \boldsymbol{r}'\right|^3} \rho(\boldsymbol{r}') d\boldsymbol{r}'. \tag{12.23}$$

However, it is usually simpler to calculate the potential

$$V(\boldsymbol{r}) = \frac{1}{4\pi\varepsilon_0} \int \frac{1}{\left|\boldsymbol{r} - \boldsymbol{r}'\right|} \rho(\boldsymbol{r}') d\boldsymbol{r}' \tag{12.24}$$

first and then calculate the electric field from

$$\boldsymbol{E} = -\nabla V. \tag{12.25}$$

This might in some situations, where do do not necessarily know ρ but only the total amount of charge, also be to tough to handle analytically. In situations like these it is better to use Poisson's equation

$$\nabla^2 V = -\frac{1}{\varepsilon_o} \rho, \tag{12.26}$$

which together with appropriate boundary conditions, is equivalent to Eq.(12.24). Very often, we are interested in finding the potential containing no charge (because the charge is located on the outside of our region of interest. In such cases Eq. (12.26) reduces to Laplace's equation ([2], p.110-111)

$$\nabla^2 V = 0. \tag{12.27}$$

According to the *Uniqueness Theorems*, the solution to Laplace's equation is uniquely determined in some volume if the potential is specified on the boundary of the volume. This easily extends to Poisson's equation by further requiring, in addition to the potential on the boundary, that the charge distribution throughout the region is known.

When considering conductors, charge are allowed to move freely and might start to rearrange themselves, leading to the *Second uniqueness theorem*, which states that the potential in a given volume, surrounded by conductors is uniquely determined if the total charge on each conductor is given.

The uniqueness theorem grants an enlarged mathematical freedom in the approach of finding the potential of a region of space. This is because the boundary uniquely determines the potential in the region enclosed region and any approach giving the correct boundary conditions would give you the correct potential function through Laplace's equation Eq. (12.27). This allows the use of tricks, like for example the classical *method of images* ([2], p.116-121).

REFERENCES

[1] D. Bedeaux, J. Vlieger, *Optical Properties of Surfaces*, Imperial College Press, London, 2001